IEEE Access
Multidisciplinary ⋮ Rapid Review ⋮ Open Access Journal

Received October 15, 2020, accepted November 6, 2020, date of publication November 16, 2020,
date of current version December 10, 2020.

Digital Object Identifier 10.1109/ACCESS.2020.3038150

A Proportional Derivative (PD) Controller for Suppression the Vibrations of a Contact-Mode AFM Model

Y. S. HAMED[1,2], K. M. ALBOGAMY[1], AND M. SAYED[2]
[1]Department of Mathematics and Statistics, College of Science, Taif University, Taif 21944, Saudi Arabia
[2]Department of Physics and Engineering Mathematics, Faculty of Electronic Engineering, Menoufia University, Menouf 32952, Egypt

Corresponding author: Y. S. Hamed (yasersalah@tu.edu.sa; eng_yaser_salah@yahoo.com)

This work was supported by Taif University researchers supporting Taif University, Taif, Saudi Arabia, under Project TURSP-2020/155.

ABSTRACT The nonlinear dynamics control of a contact-mode atomic force microscopy (AFM) system with multi forces (harmonic and parametric excitation force) utilizing the time delay proportional derivative (PD) controller is investigated. The perturbation method is utilized to calculate the first-order approximate solutions for the AFM system. The stability of the AFM system is investigated at the worst resonance case by Lyapunov's first method. We also show the bifurcation diagrams of response curves using frequency response equations before and after control are performed. Furthermore, we focus on the effect of the time-delayed control and returns signals gain on the vibration amplitude and the stability analysis of the controlled system in primary, sub-harmonic resonance for different parameter variations. In addition, the numerical results are procured using MATLAB program. Eventually, validation curves are presented to estimate the nearness degree between the analytical predictions also numerical simulation. The obtained results exhibited that, the time-delayed PD control efficiency to put down the nonlinear oscillations of the system.

INDEX TERMS A contact-mode AFM model, vibrations, proportional derivative control (PD).

NOMENCLATURE

$u, \dot{u}, \ddot{u}, \mu_1, \beta, \beta_1, \beta_2, \omega_1, \Omega_1, \Omega_2, f_1$	Dimensionless displacement, velocity, acceleration, damping coefficient, nonlinear parameters, natural and excitation frequencies and force amplitude of AFM model.
p, d	Dimensionless proportional and derivative control gains.
a	Dimensionless amplitude of AFM model.
τ_1, τ_2, t	Dimensionless signals of time-delayed controller and time.
$\sigma_1, \sigma_2, \varepsilon$	Detuning and perturbation parameters ($0 < \varepsilon \ll 1$).

I. INTRODUCTION

The Atomic force microscopy (AFM) is a powerful method that can picture almost any kind of surface, inclusive glass, polymers, ceramics, composites, and biological models. AFM is applied to measurement and locate many excitations, inclusive adhesion strength, magnetic forces, and mechanical characteristic. The AFM has three major abilities: topographic imaging, force measurement, and manipulation. Binning and Quate [1] concerned with the measure of ultrasmall excitations on particles as tiny as unattached atoms. They proposed to do this by monitoring the elastic distortion of different kinds of springs with the wiping tunneling microscope. Berg and Briggs [2] investigated intermittent contact system AFM from the viewpoint that the nonlinearity inserted by the drastic increasing the hardness on impact from that of the cantilever to that of the tip sample connect is important to its dynamics. Rützel *et al.* [3] investigated the near-resonant, nonlinear dynamic response of microcantilevers in AFM through numerical methods and simulations of discretized systems interactive with a sample through a Lennard-Jones potential. Moreover, the outcomes predict a broad range of nonlinear dynamic phenomena, many of that have been shown up on experimental AFM. A theoretical framework and an experimental procedure are presented by Abdel-Rahman and Nayfeh [4] to extend the

The associate editor coordinating the review of this manuscript and approving it for publication was Hui Xie.

applicability of acoustic/ultrasonic AFM to public contact conditions. They used multiple perturbation method to get approximating expressions of the response of the probe to one-half subharmonic resonance. Arafat *et al.* [5] used AFM to estimate material and surface properties. The multiple scales technique is applied to obtain approximate solution to the probe response in the existence of 2:1 autoparametric resonance between the second and third modes. They found that the effectiveness of the interaction extends over a considerable domain of the tip-sample model hardness. Yamasue and Hikihara [6] proposed stabilization of the chaotic microcantilever vibrations applying the method of time-delayed feedback control, that has the ability to stabilize unstable periodic orbitals embedded in chaotic attractants. Besides, they discuss an improved transient response of vibration that allows us to accelerate the scanning average of the microscopes without decreasing their amplitude sensitivity. Active control of a tapping mode AFM system via delayed feedback technique is illustrated by Salarieh and Alasty [7]. They obtained the gain of feedback and adapted according to a minimize entropy algorithm. Moreover, results simulation explains the feasibility of the proposed technique in using the method of delayed feedback for chaos control of the AFM system. Yamasue *et al.* [8] illustrated the stabilization of first experimental of non-periodic and irregular vibration of cantilever in the modulation amplitude AFM applying the time-delayed feedback controller. Bahrami and Nayfeh [9] investigated the nonlinear dynamics of an AFM cantilever through different numerical simulations achieved for a large domain of the amplitude and excitation frequency.

The hysteresis suppression and frequency response shift of contact mode AFM is illustrated by [10] applying parametric modification of the contact hardness. They used multiple perturbation technique and direct partition of motion to get the corresponding slow flow and the slow dynamic of the model, respectively. Kirrou and Belhaq [11], [12] studied analytically the effect of fast contact stiffness modulation on the frequency curve about 2:1 subharmonic resonance and primary resonance in contact-mode AFM. They give a comparison between the analytical and numerical solutions and provided example on the application to a real AFM. Bahrami and Nayfeh [13] investigated the nonlinear dynamics of an AFM microcantilever when it works in the tapping model and the AFM tip is at first existing in the bistable static zone. The differential quadrature techniques are applied to memorizes the microcantilever equation and simulate the static, free vibration responses of the scanning probe. Kirrou and Belhaq [14] investigated the control of bistability in non-contact system AFM excited by a harmonic excitation and in the existence of time-delayed feedback. Vatankhah [15] illustrated the nonlinear oscillation of an AFM with an assembled cantilever probe. The results obtained shows the model becomes more nonlinear as increases the length of the vertical extension. Hsieh *et al.* [16] studied the control and nonlinear behavior of AFM system. The numerical results showed that the tools applied for the analysis give consistent results and that changes in frequency excitation have a major influence on system behavior. Mahmoudi *et al.* [17] used the harmonic balance technique to obtain the initial-boundary problem dominant the motion of microcantilever AFM system. Wagner [18] studied the effect of external excitations on the motion of the tip in dynamic AFM. Special emphasis is placed on discussing tip response in high damping environments, such as ambient or liquid environments. The authors [19]–[27] investigated the vibration control with stability analysis of many engineering systems, particularly from string-beam, rotor blade flapping, electromechanical oscillator, rotor seal, pitch-roll motion, articulated beam, buckled beam, a cantilever beam, mitigate lateral oscillations of a vertically Jeffcott rotor system. The authors [28]–[32] were analyzed vibration performance, stability and used the proportional derivative and positive position feedback controller to reduce the vibrations of the compressor blade, offshore wind turbine tower and vertical conveyor systems.

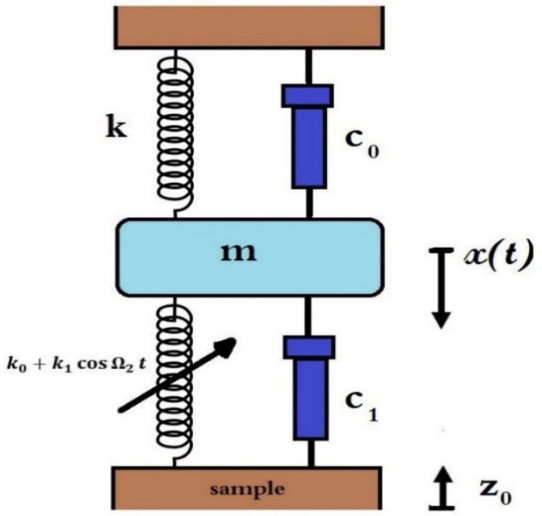

FIGURE 1. Schematic model of a tip-sample AFM.

In this article, a PD controller is applied to eliminate the oscillations of a contact mode AFM system excited by multi excitation forces. A multiple scale perturbation technique is carried out to extract resonance cases and approximate nonlinear oscillations for the AFM model. Besides, the effects of proportional control and derivative control gains on the dynamical behaviors and stability of the AFM model are obtained. Verification curves show a good agreement between numerical simulation and analytical solution.

II. SYSTEM MODELLING

Figure 1, illustrates the lumped parameter single degree of freedom AFM model with modulation of fast contact hardness. The motion equation of the system is obtained from Ref. [11], [12] and described by the following equations:

$$\ddot{u}+\varepsilon\mu_1\dot{u}+\omega_1^2u+\varepsilon\beta_1u^2+\varepsilon\beta_2u^3 + \varepsilon r\left(\frac{3}{2}\beta-\beta u+\beta_1u^2+\beta_2u^3\right)cos\,(\Omega_2t)=\varepsilon f_1cos(\Omega_1t) \quad (1)$$

Applying the time delay with the proportional derivative controller (PD) to the motion equation (1), we get the modified normalized equation as follows:

$$\begin{aligned}&\ddot{u}+\varepsilon\mu_1\dot{u}+\omega_1^2u+\varepsilon\beta_1u^2+\varepsilon\beta_2u^3\\&\quad+\varepsilon r\left(\frac{3}{2}\beta-\beta u+\beta_1u^2+\beta_2u^3\right)cos(\Omega_2t)\\&\quad=\varepsilon f_1cos\left(\Omega_1t\right)-\varepsilon pu\left(t-\tau_1\right)-\varepsilon d\dot{u}\left(t-\tau_2\right)\end{aligned}\tag{2}$$

III. MATHEMATICAL ANALYSIS

The multiple scale perturbation (MSP) [33], [34] is applied to find the approximate solutions in addition to frequency response equations respectively. To get the approximate solutions for equation (2) we applied this technique and the solution to be in the form:

$$\left.\begin{aligned}&u\left(t;\varepsilon\right)=u_0\left(T_0,T_1\right)+\varepsilon u_1\left(T_0,T_1\right)+O\left(\varepsilon^2\right)\\&u\left(t-\tau_1;\varepsilon\right)=u_{0\tau_1}\left(T_0-\tau_1,T_1-\varepsilon\tau_1\right)\\&+\varepsilon u_{1\tau_1}\left(T_0-\tau_1,T_1-\varepsilon\tau_1\right)\\&+O\left(\varepsilon^2\right)\\&u\left(t-\tau_2;\varepsilon\right)=u_{0\tau_2}\left(T_0-\tau_2,T_1-\varepsilon\tau_2\right)\\&+\varepsilon u_{1\tau_2}\left(T_0-\tau_2,T_1-\varepsilon\tau_2\right)\\&+O\left(\varepsilon^2\right)\end{aligned}\right\}\tag{3}$$

We proposed the derivatives in the format

$$\left.\begin{aligned}&\frac{d}{dt}=D_0+\varepsilon D_1\\&\frac{d^2}{dt^2}=D_0^2+2\varepsilon D_0D_1\end{aligned}\right\}\tag{4}$$

where $D_n=\frac{\partial}{\partial T_n}$, $(n=0,1)$, where D_n are the derivatives and $T_n=\varepsilon^nt$ are the time scales. Inserting equations (3) and (4) in equation (2), we equating the coefficients of powers of ε and we have

$$order(\varepsilon^0)$$
$$\left(D_0^2+\omega_1^2\right)u_0=0\tag{5}$$
$$order(\varepsilon)$$
$$\begin{aligned}&\left(D_0^2+\omega_1^2\right)u_1=-2D_0D_1u_0-\mu_1D_0u_0-\beta_1u_0^2-\beta_2u_0^3\\&+\left(r\beta u_0-\frac{3r\beta}{2}-r\beta_2u_0^3\ -r\beta_1u_0^2\right)cos(\Omega_2t)\\&+f_1cos(\Omega_1t)-pu_{0\tau_1}-dD_0u_{0\tau_2}\end{aligned}\tag{6}$$

Can be formulating the general solution for equation (5) as:

$$u_0=A_0(T_1)\,e^{i\omega_1T_0}+\bar{A}_0\left(T_1\right)e^{-i\omega_1T_0}\tag{7}$$

According to equation (7), the time-delayed solutions can be written as:

$$u_{0\tau_1}=A_0(T_1-\varepsilon\tau_2)\,e^{i\omega_1(T_0-\tau_1)}+\bar{A}_0\left(T_1-\varepsilon\tau_2\right)e^{-i\omega_1(T_0-\tau_1)}\tag{8a}$$

$$u_{0\tau_2}=A_0(T_1-\varepsilon\tau_2)\,e^{i\omega_1(T_0-\tau_2)}+\bar{A}_0\left(T_1-\varepsilon\tau_2\right)e^{-i\omega_1(T_0-\tau_2)}\tag{8b}$$

where $A_0\left(T_1\right)$ and $\bar{A}_0\left(T_1\right)$ are unknown functions in T_1.

Expanding $A_{0\tau_1}$ and $A_{0\tau_2}$ in Taylor-series as:

$$A_{0\tau_1}=A_0\left(T_1\right)+\frac{\varepsilon\tau_1}{1!}D_1A_0\left(T_1\right)+\ldots=A_0\left(T_1\right)\tag{9a}$$

$$A_{0\tau_2}=A_0\left(T_1\right)+\frac{\varepsilon\tau_2}{1!}D_1A_0\left(T_1\right)+\ldots=A_0\left(T_1\right)\tag{9b}$$

Taking equation (9) into account, substituting equations (7) and (8) into equation (6), we get:

$$\begin{aligned}&\left(D_0^2+\omega_1^2\right)u_1\\&=\left(-2i\omega_1D_1A_0-i\mu_1\omega_1A_0-3\beta_2A_0^2\bar{A}_0\right)e^{i\omega_1T_0}\\&+2i\omega_1D_1\bar{A}_0+i\mu_1\omega_1\bar{A}_0+\left(3\beta_2\bar{A}_0^2A_0\right)e^{-i\omega_1T_0}\\&-p\left(A_0e^{i\omega_1T_0}e^{-i\omega_1\tau_1}+\bar{A}_0e^{-i\omega_1T_0}e^{i\omega_1\tau_1}\right)\\&-id\omega_1\left(A_0e^{i\omega_1T_0}e^{-i\omega_1\tau_2}+\bar{A}_0e^{-i\omega_1T_0}e^{i\omega_1\tau_2}\right)\\&-\left(r\beta_1A_0\bar{A}_0+r\frac{3\beta}{4}\right)\left(e^{i\Omega_2T_0}\ +e^{-i\Omega_2T_0}\right)\\&-\left(\beta_1A_0^2e^{2i\omega_1T_0}+\beta_1\bar{A}_0^2e^{-2i\omega_1T_0}\right)\\&-\left(\beta_2A_0^3e^{3i\omega_1T_0}+\beta_2\bar{A}_0^3e^{3i\omega_1T_0}\right)\\&+\frac{f_1}{2}\left(e^{i\Omega_1T_0}+e^{-i\Omega_1T_0}\right)-\left(\frac{3r\beta_2}{2}A_0\bar{A}_0-\frac{r\beta}{2}\right)\\&\times A_0e^{i(\Omega_2+\omega_1)T_0}-\left(\frac{3r\beta_2}{2}A_0\bar{A}_0-\frac{r\beta}{2}\right)\\&\times\bar{A}_0e^{-i(\Omega_2+\omega_1)T_0}-\left(\frac{3r\beta_2}{2}\bar{A}_0A_0-\frac{r\beta}{2}\right)\\&\times\bar{A}_0e^{i(\Omega_2-\omega_1)T_0}-\left(\frac{3r\beta_2}{2}\bar{A}_0A_0-\frac{r\beta}{2}\right)\\&\times A_0e^{-i(\Omega_2-\omega_1)T_0}\\&-\left(\frac{r\beta_1}{2}A_0^2e^{i(\Omega_2+2\omega_1)T_0}+\frac{r\beta_1}{2}\bar{A}_0^2e^{-i(\Omega_2+2\omega_1)T_0}\right)\\&-\left(\frac{r\beta_1}{2}\bar{A}_0^2e^{i(\Omega_2-2\omega_1)T_0}+\frac{r\beta_1}{2}A_0^2e^{-i(\Omega_2-2\omega_1)T_0}\right)\\&-\left(\frac{r\beta_2}{2}A_0^3e^{i(\Omega_2+3\omega_1)T_0}+\frac{r\beta_2}{2}\bar{A}_0^3e^{-i(\Omega_2+3\omega_1)T_0}\right)\\&-\left(\frac{r\beta_2}{2}\bar{A}_0^3e^{i(\Omega_2-3\omega_1)T_0}+\frac{r\beta_2}{2}A_0^3e^{-i(\Omega_2-3\omega_1)T_0}\right)\\&-\beta_1A_0\bar{A}_0\end{aligned}\tag{10}$$

For abounded solution, we eliminated the secular terms $e^{\pm i\omega_1T_0}$ and the solutions of equation (10) obtained as:

$$\begin{aligned}u_1=&A_1e^{i\omega_1T_0}+\bar{A}_1e^{-i\omega_1T_0}-\frac{1}{\left(\omega_1^2-\Omega_2^2\right)}\\&\times\left(r\beta_1A_0\bar{A}_0+r\frac{3\beta}{4}\right)\left(e^{i\Omega_2T_0}+e^{-i\Omega_2T_0}\right)\\&+\frac{\beta_1}{3\omega_1^2}\left(A_0^2e^{2i\omega_1T_0}+\bar{A}_0^2e^{-2i\omega_1T_0}\right)+\frac{\beta_2}{8\omega_1^2}\\&\times\left(A_0^3e^{3i\omega_1T_0}+\bar{A}_0^3e^{-3i\omega_1T_0}\right)\\&-\frac{r}{2\left(\omega_1^2-\left(\Omega_2+\omega_1\right)^2\right)}\\&\times\left(\left(3\beta_2A_0^2\bar{A}_0-\beta A_0\right)e^{i(\Omega_2+\omega_1)T_0}\right.\\&\left.+\left(3\beta_2\bar{A}_0^2A_0\ -\beta\bar{A}_0\right)e^{-i(\Omega_2+\omega_1)T_0}\right)\end{aligned}$$

$$
\begin{aligned}
&- \frac{r}{2\left(\omega_1^2-(\Omega_2-\omega_1)^2\right)} \\
&\times \left(\left(3\beta_2\bar{A}_0^2A_0-\beta\bar{A}_0\right)e^{i(\Omega_2-\omega_1)T_0}\right. \\
&\left.+\left(3\beta_2\bar{A}_0A_0-\beta\right)A_0e^{-i(\Omega_2-\omega_1)T_0}\right) \\
&- \frac{r\beta_1}{2\left(\omega_1^2-(\Omega_2+2\omega_1)^2\right)} \\
&\times \left(A_0^2e^{i(\Omega_2+2\omega_1)T_0}+\bar{A}_0^2e^{-i(\Omega_2+2\omega_1)T_0}\right) \\
&- \frac{r\beta_1}{2\left(\omega_1^2-(\Omega_2-2\omega_1)^2\right)} \\
&\times \left(\bar{A}_0^2e^{i(\Omega_2-2\omega_1)T_0}+A_0^2e^{-i(\Omega_2-2\omega_1)T_0}\right) \\
&- \frac{r\beta_2}{2\left(\omega_1^2-(\Omega_2+3\omega_1)^2\right)} \\
&\times \left(A_0^3e^{i(\Omega_2+3\omega_1)T_0}+\bar{A}_0^3e^{-i(\Omega_2+3\omega_1)T_0}\right) \\
&- \frac{r\beta_2}{2\left(\omega_1^2-(\Omega_2-3\omega_1)^2\right)} \\
&\times \left(\bar{A}_0^3e^{i(\Omega_2-3\omega_1)T_0}+A_0^3e^{-i(\Omega_2-3\omega_1)T_0}\right) \\
&+ \frac{f_1}{2\left(\omega_1^2-\Omega_1^2\right)}\left(e^{i\Omega_1T_0}+e^{-i\Omega_1T_0}\right)-\frac{\beta_1}{\omega_1^2}A_0\bar{A}_0
\end{aligned}
\tag{11}
$$

where A_1 and $\bar{A}_1$ are complex functions in T_1. For stability investigation, where the solution is only dependent on T_0 and T_1 at primary, sub-harmonic cases $\Omega_1 \cong \omega_1$, $\Omega_2 \cong 2\omega_1$, we introduce detuning parameters σ_1 and σ_2 such that

$$\Omega_1 = \omega_1 + \varepsilon\sigma_1, \Omega_2 = 2\omega_1 + \varepsilon\sigma_2 \tag{12}$$

From equations (10) the secular terms are removed by (equate the secular terms to zero), result in solvability conditions for the first order approach, like:

$$
\begin{aligned}
&\left(-2i\omega_1D_1A_0-i\mu_1\omega_1A_0-3\beta_2A_0^2\bar{A}_0\right)e^{i\omega_1T_0} \\
&-\left(\frac{3r\beta_2}{2}\bar{A}_0^2A_0-\frac{r\beta}{2}\bar{A}_0\right)e^{i(\Omega_2-\omega_1)T_0}-\frac{r\beta_2}{2}A_0^3e^{-i(\Omega_2-3\omega_1)T_0} \\
&+\frac{f_1}{2}e^{i\Omega_1T_0}-pA_0e^{i\omega_1T_0}e^{-i\omega_1\tau_1}-id\omega_1A_0e^{i\omega_1T_0}e^{-i\omega_1\tau_2}=0
\end{aligned}
\tag{13}
$$

Substituting equation (12) into equations (13), we obtained:

$$
\begin{aligned}
&\left(-2i\omega_1D_1A_0-i\mu_1\omega_1A_0-3\beta_2A_0^2\bar{A}_0\right)e^{i\omega_1T_0} \\
&-\left(\frac{3r\beta_2}{2}\bar{A}_0^2A_0-\frac{r\beta}{2}\bar{A}_0\right)e^{i(\omega_1+\varepsilon\sigma_2)T_0} \\
&-\frac{r\beta_2}{2}A_0^3e^{i(\omega_1-\varepsilon\sigma_2)T_0}+\frac{f_1}{2}e^{i(\omega_1+\varepsilon\sigma_1)T_0} \\
&-pA_0e^{i\omega_1T_0}e^{-i\omega_1\tau_1}-id\omega_1A_0e^{i\omega_1T_0}e^{-i\omega_1\tau_2}=0
\end{aligned}
\tag{14}
$$

Dividing equation (14) by $e^{i\omega_1T_0}$ we obtained:

$$
\begin{aligned}
&-2i\omega_1D_1A_0-i\mu_1\omega_1A_0-3\beta_2A_0^2\bar{A}_0 \\
&-\left(\frac{3r\beta_2}{2}\bar{A}_0^2A_0-\frac{r\beta}{2}\bar{A}_0\right)e^{i\sigma_2T_1}-\frac{r\beta_2}{2}A_0^3e^{-i\sigma_2T_1} \\
&+\frac{f_1}{2}e^{i\sigma_1T_1}-pA_0e^{-i\omega_1\tau_1}-id\omega_1A_0e^{-i\omega_1\tau_2}=0
\end{aligned}
\tag{15}
$$

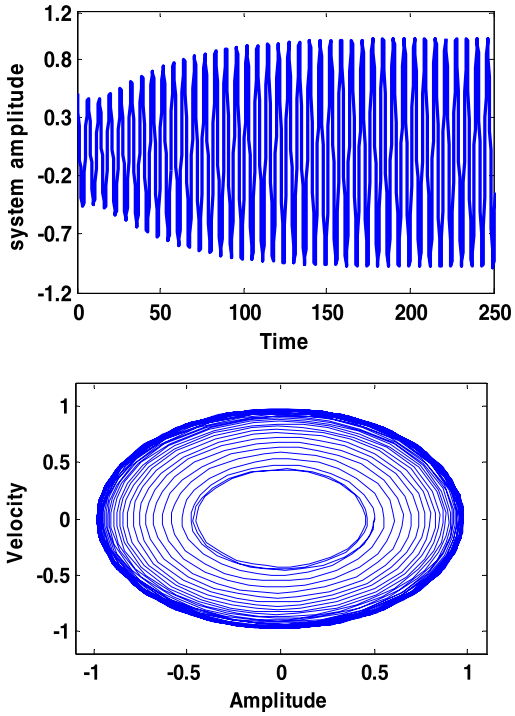

FIGURE 2. Response and phase plane of the uncontrolled AFM system at $\Omega_1 \cong \omega_1$, $\Omega_2 \cong 2\omega_1$.

Substituting the polar forms

$$A_0 = \frac{1}{2}ae^{i\varphi(T_1)}, \tag{16}$$

where a and φ are the amplitude and phase of the system. Inserting equation (16) in equation (15), we obtained the first order differential equations:

$$
\begin{aligned}
\dot{a} = &-\frac{1}{2}\mu_1a-\frac{1}{8\omega_1}r\beta_2a^3\sin\theta_2+\frac{1}{4\omega_1}r\beta a\sin\theta_2 \\
&+\frac{f_1}{2\omega_1}\sin\theta_1+\frac{1}{2\omega_1}pa\sin(\omega_1\tau_1)-\frac{1}{2}da\cos(\omega_1\tau_2)
\end{aligned}
\tag{17}
$$

$$
\begin{aligned}
\dot{\theta}_1 = &\sigma_1-\frac{3}{8\omega_1}\beta_2a^2-\frac{1}{4\omega_1}r\beta_2a^2\cos2\theta_1+\frac{1}{4\omega_1}r\beta\cos2\theta_1 \\
&+\frac{f_1}{2a\omega_1}\cos\theta_1-\frac{1}{2\omega_1}p\cos(\omega_1\tau_1)-\frac{1}{2}d\sin(\omega_1\tau_2)
\end{aligned}
\tag{18}
$$

where

$$\theta_1 = \sigma_1T_1-\varphi, \theta_2 = \sigma_2T_1-2\varphi, \dot{\varphi} = \sigma_1-\dot{\theta}_1, \theta_2 = 2\theta_1,$$

IV. STABILITY INVESTIGATION

We put $\dot{a} = \dot{\theta}_1 = 0$, into equations (17) and (18), to get the steady state as:

$$
\begin{aligned}
\frac{1}{2}\mu_1a = &-\frac{1}{8\omega_1}r\beta_2a^3sin\theta_2+\frac{1}{4\omega_1}r\beta asin\theta_2 \\
&+\frac{f_1}{2\omega_1}sin\theta_1+\frac{1}{2\omega_1}pasin(\omega_1\tau_1) \\
&-\frac{1}{2}dacos(\omega_1\tau_2)
\end{aligned}
\tag{19}
$$

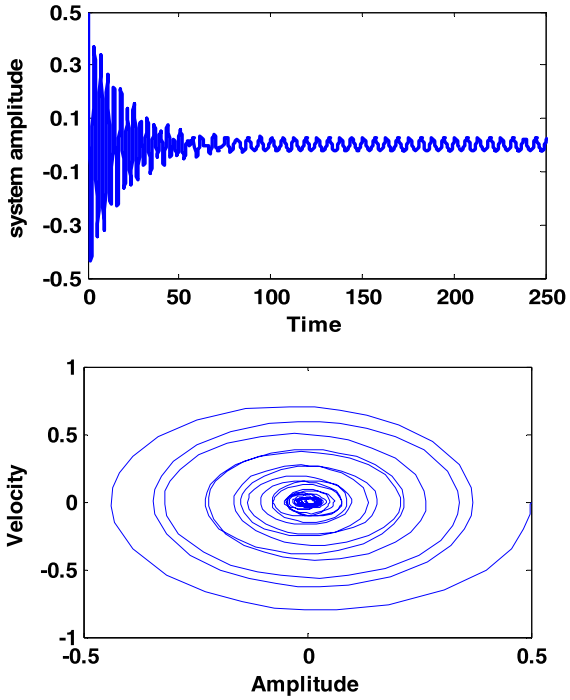

FIGURE 3. Response and phase plane of the controlled AFM system at $\Omega_1 \cong \omega_1, \Omega_2 \cong 2\omega_1, p = 2, d = 0.05, \tau_1 = \tau_2 = 0$.

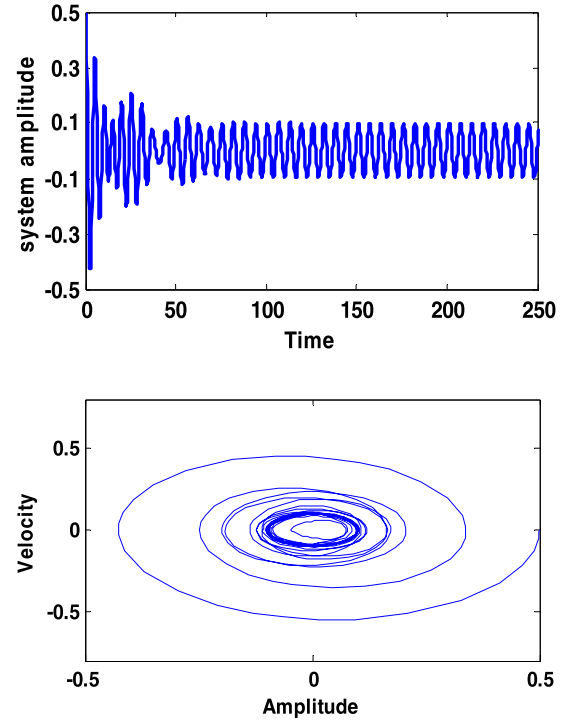

FIGURE 4. Response and phase plane of the controlled AFM system at $\Omega_1 \cong \omega_1, \Omega_2 \cong 2\omega_1, p = .5, d = .05, \tau_1 = \tau_2 = 0$.

$$\sigma_1 a - \frac{3}{8\omega_1}\beta_2 a^3 = \frac{1}{4\omega_1} r\beta_2 a^3 cos2\theta_1 - \frac{1}{4\omega_1} r\beta a cos2\theta_1 - \frac{f_1}{2\omega_1} cos\theta_1 + \frac{1}{2\omega_1} pacos(\omega_1\tau_1) + \frac{1}{2} dasin(\omega_1\tau_2) \quad (20)$$

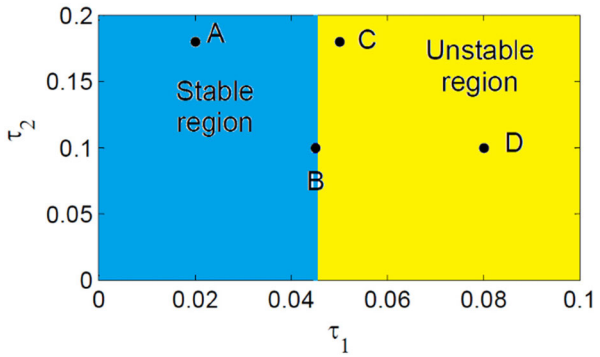

FIGURE 5. Effects of time-delayed on the stable solution region in plane of $\tau_1 - \tau_2$.

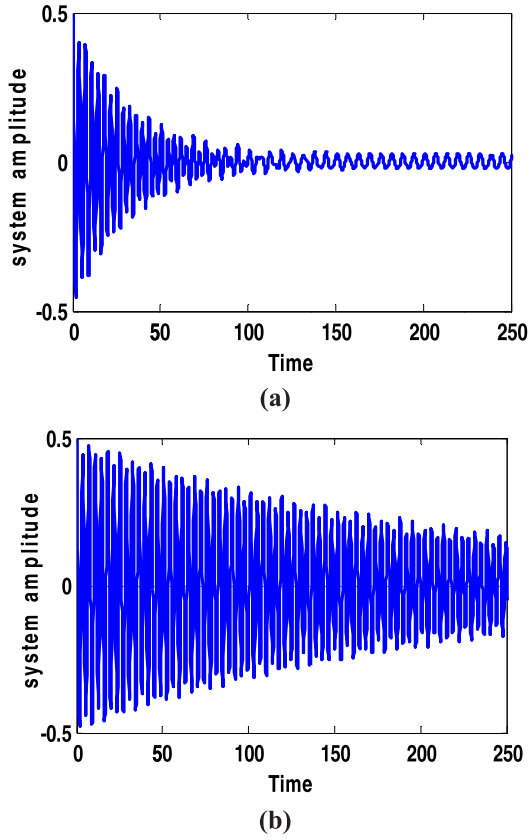

FIGURE 6. Response of the controlled AFM model. (a) $\tau_1 = 0.02$, $\tau_2 = 0.18$ (According to point A in Figure 5) (b) $\tau_1 = 0.045$, $\tau_2 = 0.1$ (According to point B in Figure 5).

To check the stability of the nonlinear solution based on Lyapunov's direct method [34], we suppose that

$$a = a_{10} + a_{11}, \quad \text{and } \theta_1 = \theta_{10} + \theta_{11} \quad (21)$$

where a_{10} and θ_{10} are the solutions of equations (17) and (18). Inserting equation (21) into equations (17), (18), and using only linear terms in a_{11} and θ_{11}, we obtain the system of differential equations

$$\dot{a}_{11} = \left(-\frac{\mu_1}{2} - \frac{3r\beta_2}{8\omega_1} a_{10}^2 sin(2\theta_{10}) + \frac{r\beta}{4\omega_1} sin(2\theta_{10}) + \frac{1}{2\omega_1} psin(\omega_1\tau_1) - \frac{1}{2} dcos(\omega_1\tau_2)\right) a_{11}$$

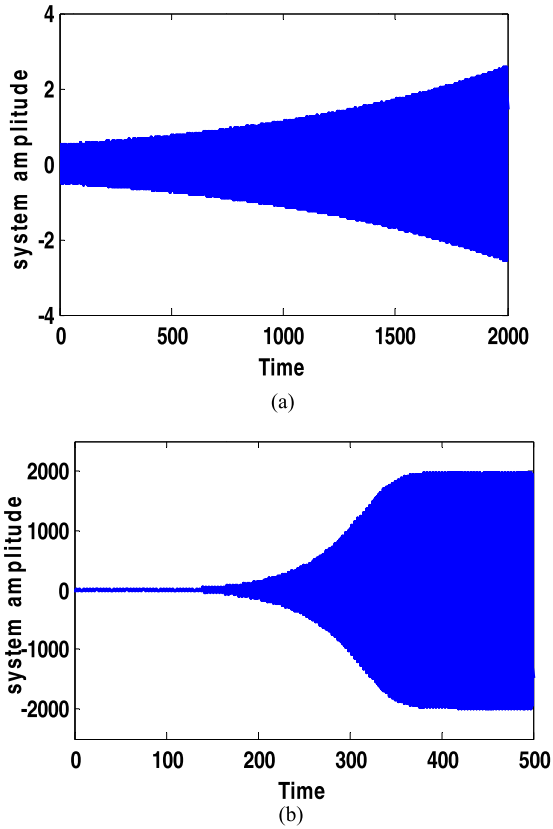

FIGURE 7. Response of the controlled AFM model. (c) $\tau_1 = 0.05$, $\tau_2 = 0.18$ (According to point C in Figure. 5). (d) $\tau_1 = 0.08$, $\tau_2 = 0.1$ (According to point D in Figure. 5).

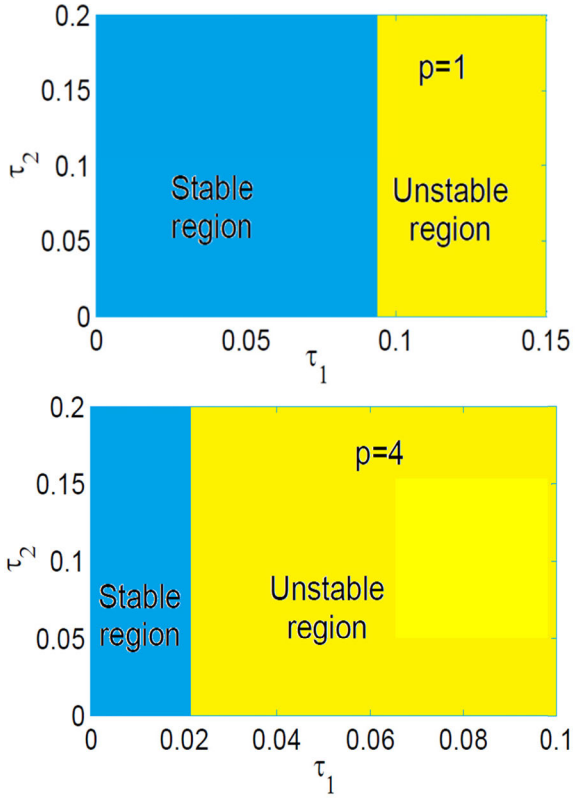

FIGURE 8. Effects of the control signal gain p on the stable solution region in plane of $\tau_1 - \tau_2$.

$$+\left(\frac{f_1}{2\omega_1}cos\theta_{10} + \frac{r\beta}{2\omega_1}a_{10}cos\,(2\theta_{10}) - \frac{r\beta_2}{4\omega_1}a_{10}^3cos\,(2\theta_{10})\right)\theta_{11} \quad (22)$$

$$\dot{\theta}_{11} = \left(-\frac{3\beta_2}{4\omega_1}a_{10} - \frac{f_1}{2\omega_1 a_{10}^2}cos\theta_{10} - \frac{r\beta_2}{2\omega_1}a_{10}cos\,(2\theta_{10})\right) \times a_{11} + \left(\frac{r\beta_2}{2\omega_1}a_{10}^2 sin\,(2\theta_{10}) - \frac{r\beta}{2\omega_1}sin\,(2\theta_{10}) - \frac{f_1}{2\omega_1 a_{10}}sin\theta_{10}\right)\theta_{11} \quad (23)$$

we can be express the above system in a matrix form as follows

$$\begin{pmatrix}\dot{a}_{11}\\ \dot{\theta}_{11}\end{pmatrix} = \begin{pmatrix}\Gamma_1 & \Gamma_2\\ \Gamma_3 & \Gamma_4\end{pmatrix}\begin{pmatrix}a_{11}\\ \theta_{11}\end{pmatrix} \quad (24)$$

where a_{11} and θ_{11} are arbitrary real functions of T_1.

The eigen-values of the above system is

$$\begin{vmatrix}\Gamma_1 - \lambda & \Gamma_2\\ \Gamma_3 & \Gamma_5 - \lambda\end{vmatrix} = 0 \quad (25)$$

$$\text{i.e. } \lambda^2 + r_1\lambda + r_2 = 0 \quad (26)$$

where r_1 and r_2 are functions of the parameters (a, ω_1,σ_1,f_1, μ_1, p,d, r, β,β_2, θ_{10}, τ_1, τ_2). Based on Routh–Huriwitz criterion, the necessary and sufficient conditions that the system is stable, if the roots of equation (31) have negative real parts, and the following equation is verified:

$$r_1 > 0, \quad r_1 r_2 > 0 \quad (27)$$

V. DISCUSSIONS AND NUMERICAL RESULTS

This section investigated the time history, bifurcation diagram and validation the numerical results with the analytical ones for the contact-mode AFM model before and after adding controller at the dimensionless system parameters of equations (2) as: $\mu_1 = 0.05$, $\beta = 0.01$,$\beta_1 = 0.005$,$\beta_2 = 0.0004$, $r = 0.2$,$\omega_1 = 1$,$\Omega_1 = 1$,$\Omega_2 = 2$,$f_1 = 0.05$, $p = 2.0$,$d = 0.05$.

A. SYSTEM WITH CONTROLLER

Figure 3 represents the controlled AFM time history at $\Omega_1 \cong \omega_1, \Omega_2 \cong 2\omega_1$. With this figure, the system amplitude has been suppressed from about 1 at steady state as in Figure 2 to about 0.02 as in Figure 3 at $p = 2$, $d = 0.05$ then, the controller efficiency E_a (E_a = amplitude of uncontrolled system / amplitude of controlled system) is about **50**. Then the AFM vibration reduced by about **98%**.

From Figure 4, we show that the amplitude has been suppressed to about 0.1 at $\Omega_1 \cong \omega_1$, $\Omega_2 \cong 2\omega_1$,$p = 0.5$, $d = 0.05$ then, the controller efficiency E_a is about **10** and the AFM amplitude is reduced by about **90%**.

Figures 6 and 7 illustrate the controlled AFM response according to points A, B, C and D as in Figure 5. We observed

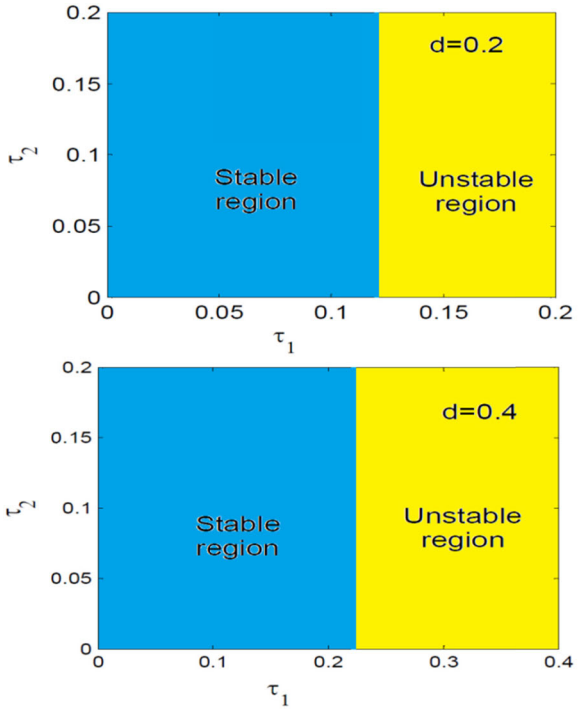

FIGURE 9. Effects of the feedback signal gain d on the stable solution region in plane of $\tau_1 - \tau_2$.

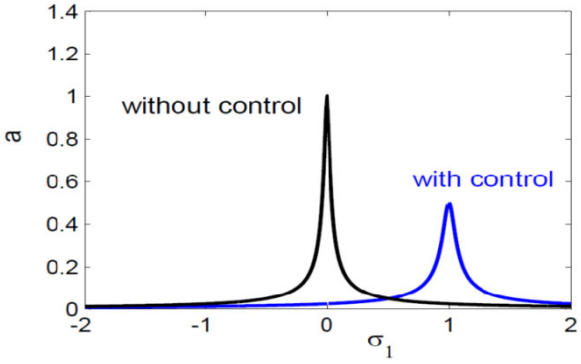

FIGURE 10. Effects of detuning parameters σ_1 on the frequency response curve.

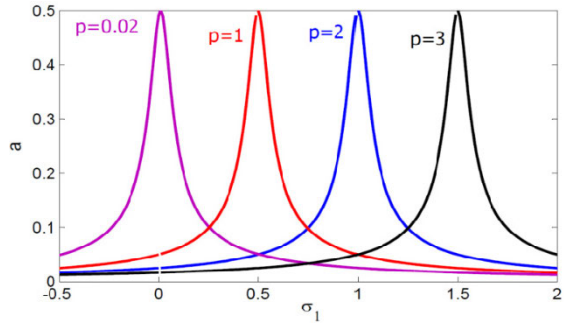

FIGURE 11. Effects of control signal gain p.

that the stable solutions located inside the stable region at the point A and Hopf curve occur at the boundary between the stable and unstable regions at B. In addition, the unstable solutions located inside the unstable region at

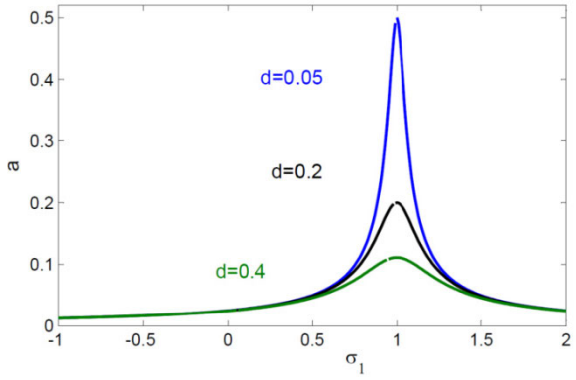

FIGURE 12. Effects of feedback signal gain d.

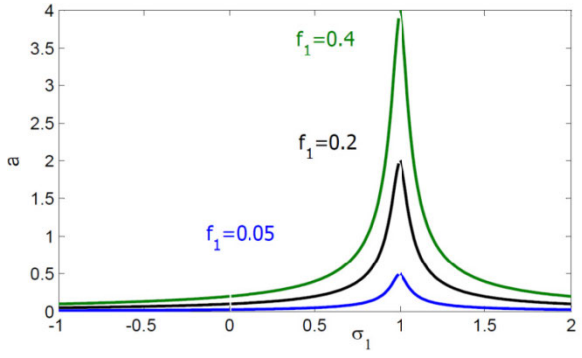

FIGURE 13. Effects of the excitation force f_1.

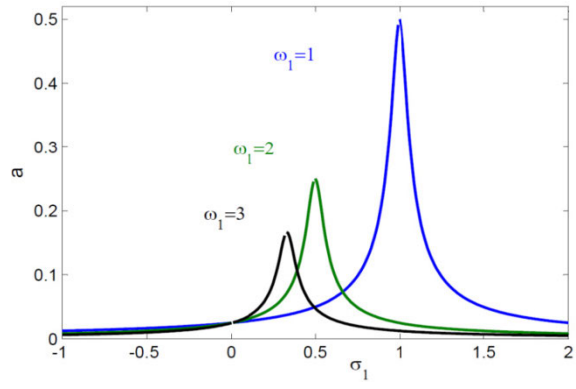

FIGURE 14. Effects of natural frequency ω_1.

the points C and D. Figure 6(a) shows stable periodic motion, quasi-periodic motion in Figure 6(b), and unstable motion in Figures 7(a, b). By comparing the data in Figure 5 with the results of Figures 6 and 7, we conclude that there is best validations between the numerical methods applied and the analytical ones.

Figure 8 shows the influents of proportional control gain p on the stable solutions region in the $\tau_1 - \tau_2$ plane. From this figure, it is clear that for decreasing the proportional control gain p, the stability region is increased. In addition, the region of stability in $\tau_1 - \tau_2$ plane is increasing, for increasing derivative control gain d, as illustrated in Figure 9.

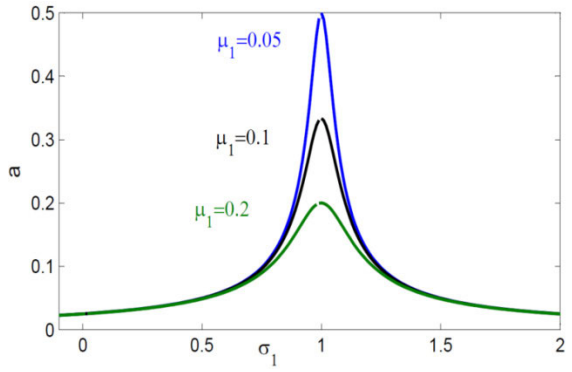

FIGURE 15. Effects of damping coefficient μ_1.

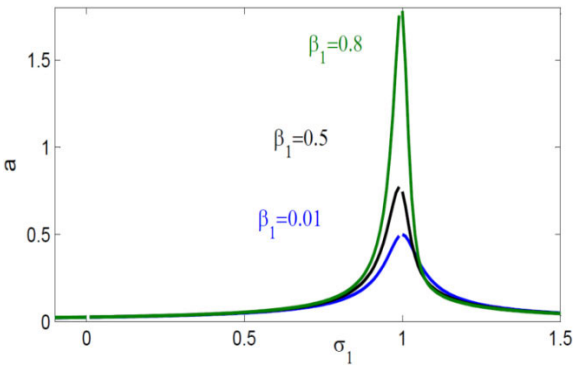

FIGURE 16. Effects of nonlinear parameter β_1.

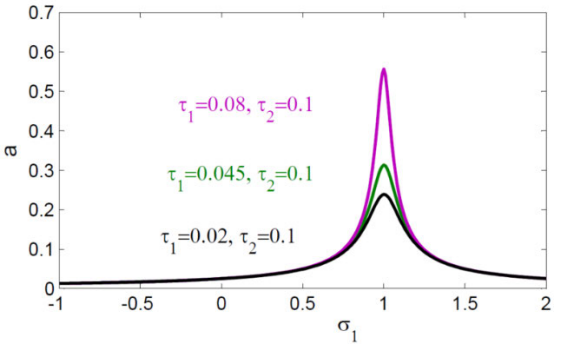

FIGURE 17. Effects of time delayed τ_1 and τ_2.

Figure 10 shows the detuning parameter σ_1 effects on frequency response curve for the system without and with control. We note that at the system without controller the maximum amplitude occurs when $\sigma_1 = 0$ ($\Omega_1 \cong \omega_1, \Omega_2 \cong 2\omega_1$) and the amplitude is about 1, while for system with control the amplitde at $\sigma_1 = 0$ is about 0.02. Then, the controller efficiency E_a is about **50** and the AFM amplitude is reduced by about **98%**. Figure 11 show that for growing control gain p the curve is moved to the right. We have inverse proportional in steady state amplitude with feedback gain d and directed proportional to the excitation force f_1 respectively as shown in Figures 12, 13.

Figures 14, 15 shows that amplitude is inversely proportional to the natural frequencies ω_1, and damping coefficient

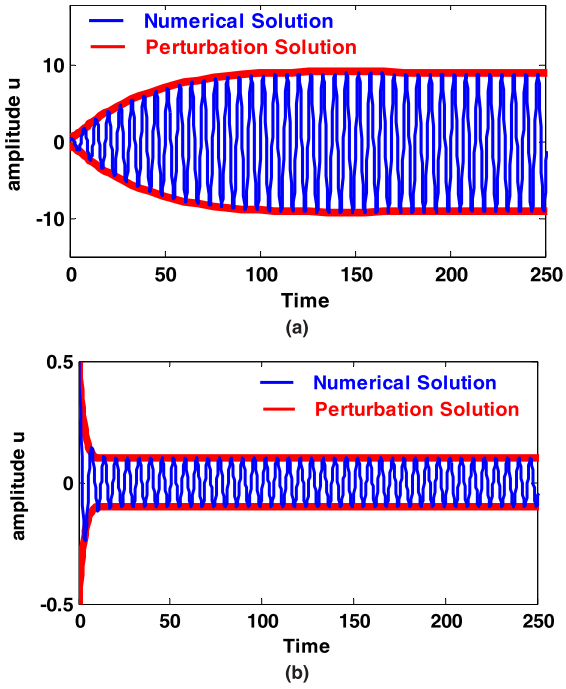

FIGURE 18. Verification curves of analytical solutions also numerical of the system (uncontrolled) at $\Omega_1 \cong \omega_1, \Omega_2 \cong 2\omega_1, p = 0, d = 0$. (a) $f_1 = 0.5, \tau_1 = \tau_2 = 0$ (b) $\mu_1 = 0.5, \tau_1 = \tau_2 = 0$.

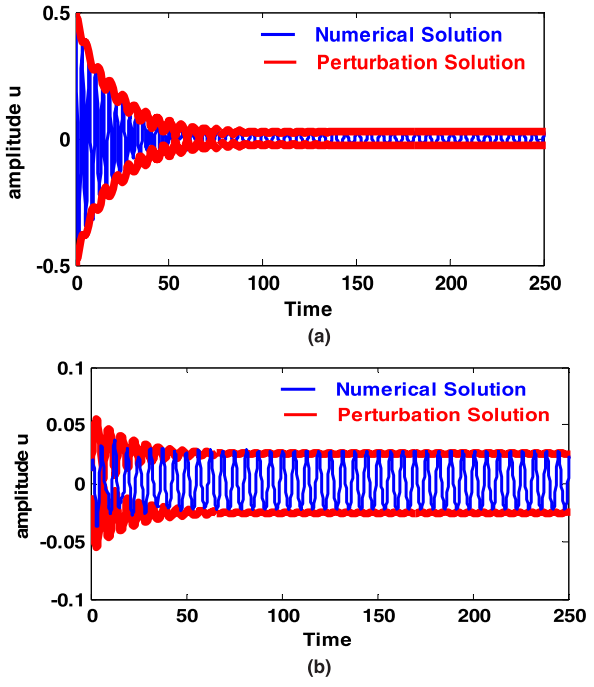

FIGURE 19. Verification curves of analytical solutions also numerical of the system (controlled) at $\Omega_1 \cong \omega_1, \Omega_2 \cong 2\omega_1, p = 2, d = 0.05$, (a) $u(0) = 0.5, \dot{u}(0) = 0$ (b) $u(0) = 0.01, \dot{u}(0) = 0.01$.

μ_1. As will, to increasing natural frequency ω_1 the curve is shifted to the right side. From growing values of nonlinear parameter β_1, the amplitude is increasing as seen in Figure 16. From Figure 17, we record that the maximum

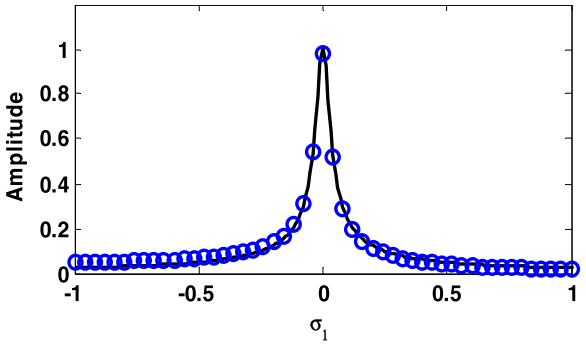

FIGURE 20. Verification curves of frequency response.

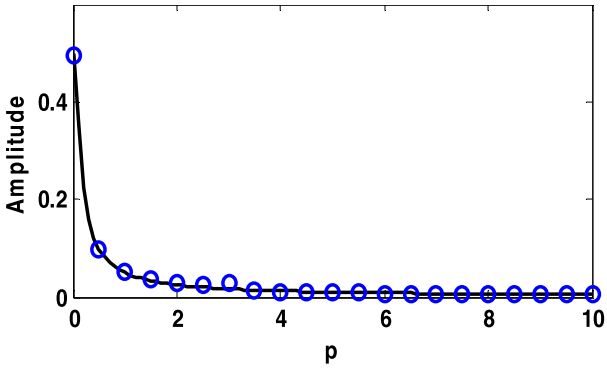

FIGURE 21. Verification of effects of control gain p.

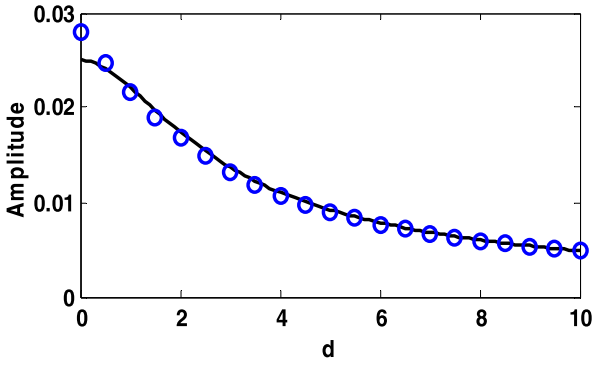

FIGURE 22. Verification of effects of control feedback d.

amplitude of is increasing with the increase at time delays τ_1 values.

B. VERIFICATION CURVES OF ANALYTICAL SOLUTIONS OF THE AFM SYSTEM

From time response, Figures 18 and 19 shown the comparison among the numerical solution for the system equation (2) applying Rung-Kutta method and perturbation modulated amplitude of equations (17)-(18) using the multiple perturbation method with different values of natural and excitation frequencies at $\Omega_1 \cong \omega_1, \Omega_2 \cong 2\omega_1$. The stiff blue line agrees with the numerical integral, while the stiff red line show to perturbation solution. With these figures, we see that the analytical solutions are fully compatible with numerical solutions. Figure 20 explain a comparison among the frequency response curves utilizing MSP method in the uncontrolled system versus σ_1 also the numerical solution applying RKM in equation (2) at values of the parameters in Figure 2.

Figures 21 and 22 shows that the validated curves of closeness between analytical and numerical solutions at different values of proportional and derivative control gains p, d.

VI. CONCLUSION

In this work, the nonlinear vibrations of the AFM model in contact mode are reduced utilizing a time-delay PD controller. The effect of different parameters before and after applying the control on frequency response curves was investigated. The control and feedback signals gain effects respecting the vibration amplitude also stability behavior of the controlled system were studied with the case $\Omega_1 \cong \omega_1$, $\Omega_2 \cong 2\omega_1$. From this study, we remark the following:

- The efficiency E_a was about 50, and controller reduced the vibration by about 98%.
- The amplitude a of the system without control reached maximum value at $\sigma_1 = 0$ ($\Omega_1 \cong \omega_1, \Omega_2 \cong 2\omega_1$) while after control the amplitude a of the system reached minimum value at $\sigma_1 = 0$, the controller is able to eliminate the vibrations.
- For increasing derivative control gain d, the stability region in $\tau_1 - \tau_2$ plane is increasing.
- For increasing proportional control gain p, the stability region in $\tau_1 - \tau_2$ plane is decreasing.
- The steady state amplitude grows with growing the values of excitation force f_1.
- The amplitude a has inverse proportional with the damping coefficient μ_1 and the natural frequency ω_1.
- for increasing the time delay τ_1, the maximum amplitudes were increasing.
- Figures 18 to 22 show that a good agreement of closeness between analytical and numerical solutions.

CONFLICTS OF INTEREST

The authors declare that there are no conflicts of interest associated with this publication.

ACKNOWLEDGMENT

This Research was supported by Taif University Researchers Supporting Project Number (TURSP-2020/155), Taif University, Taif, Saudi Arabia.

REFERENCES

[1] G. Binnig and C. F. Quate, "Atomic force microscope," *Phys. Rev. Lett.*, vol. 56, no. 9, pp. 930–933, 1986.

[2] J. Berg and G. A. D. Briggs, "Nonlinear dynamics of intermittent-contact mode atomic force microscopy," *Phys. Rev. B, Condens. Matter*, vol. 55, no. 22, pp. 14899–14908, Jun. 1997.

[3] S. Rützel, S. I. Lee, and A. Raman, "Nonlinear dynamics of atomic-force-microscope probes driven in Lennard-Jones potentials," *Proc. Math., Phys. Eng. Sci.*, vol. 459, no. 2036, pp. 1925–1948, 2003.

[4] E. M. Abdel-Rahman and A. H. Nayfeh, "Contact force identification using the subharmonic resonance of a contact-mode atomic force microscopy," *Nanotechnology*, vol. 16, no. 2, pp. 199–207, Feb. 2005.

[5] H. N. Arafat, A. H. Nayfeh, and E. M. Abdel-Rahman, "Modal interactions in contact-mode atomic force microscopes," *Nonlinear Dyn.*, vol. 54, nos. 1–2, pp. 151–166, Oct. 2008.
[6] K. Yamasue and T. Hikihara, "Control of microcantilevers in dynamic force microscopy using time delayed feedback," *Rev. Sci. Instrum.*, vol. 77, no. 5, May 2006, Art. no. 053703.
[7] H. Salarieh and A. Alasty, "Control of chaos in atomic force microscopes using delayed feedback based on entropy minimization," *Commun. Nonlinear Sci. Numer. Simul.*, vol. 14, no. 3, pp. 637–644, Mar. 2009.
[8] K. Yamasue, K. Kobayashi, H. Yamada, K. Matsushige, and T. Hikihara, "Controlling chaos in dynamic-mode atomic force microscope," *Phys. Lett. A*, vol. 373, no. 35, pp. 3140–3144, Aug. 2009.
[9] A. Bahrami and A. H. Nayfeh, "On the dynamics of tapping mode atomic force microscope probes," *Nonlinear Dyn.*, vol. 70, no. 2, pp. 1605–1617, Oct. 2012.
[10] I. Kirrou and M. Belhaq, "Frequency shift and hysteresis suppression in contact-mode AFM using contact stiffness modulation," in *Proc. MATEC Web Conf.*, vol. 1, 2012, Art. no. 04003.
[11] I. Kirrou and M. Belhaq, "Contact stiffness modulation in contact-mode atomic force microscopy," *Int. J. Non-Linear Mech.*, vol. 55, pp. 102–109, Oct. 2013.
[12] I. Kirrou and M. Belhaq, "Effect of contact stiffness modulation in contact-mode AFM under subharmonic excitation," *Commun. Nonlinear Sci. Numer. Simul.*, vol. 18, no. 10, pp. 2916–2925, Oct. 2013.
[13] A. Bahrami and A. H. Nayfeh, "Nonlinear dynamics of tapping mode atomic force microscopy in the bistable phase," *Commun. Nonlinear Sci. Numer. Simul.*, vol. 18, no. 3, pp. 799–810, Mar. 2013.
[14] I. Kirrou and M. Belhaq, "Control of bistability in non-contact mode atomic force microscopy using modulated time delay," *Nonlinear Dyn.*, vol. 81, nos. 1–2, pp. 607–619, Jul. 2015.
[15] R. Vatankhah, "Nonlinear vibration of AFM microcantilevers with sidewall probe," *J. Brazilian Soc. Mech. Sci. Eng.*, vol. 39, no. 12, pp. 4873–4886, Dec. 2017.
[16] C.-T. Hsieh, H.-T. Yau, C.-C. Wang, and Y.-S. Hsieh, "Nonlinear behavior analysis and control of the atomic force microscope and circuit implementation," *J. Low Freq. Noise, Vibrat. Act. Control*, vol. 38, nos. 3–4, pp. 1576–1593, Dec. 2019.
[17] M. S. Mahmoudi, A. Ebrahimian, and A. Bahrami, "Higher modes and higher harmonics in the non-contact atomic force microscopy," *Int. J. Non-Linear Mech.*, vol. 110, pp. 33–43, Apr. 2019.
[18] T. Wagner, "Steady-state and transient behavior in dynamic atomic force microscopy," *J. Appl. Phys.*, vol. 125, no. 4, Jan. 2019, Art. no. 044301.
[19] Y. S. Hamed, M. Sayed, D.-X. Cao, and W. Zhang, "Nonlinear study of the dynamic behavior of a string-beam coupled system under combined excitations," *Acta Mechanica Sinica*, vol. 27, no. 6, pp. 1034–1051, Dec. 2011.
[20] M. Sayed, A. A. Mousa, and D. Y. Alzaharani, "Non-linear time delay saturation controller for reduction of a non-linear vibrating system via 1:4 internal resonance," *J. Vibroeng.*, vol. 18, no. 4, pp. 2515–2536, Jun. 2016.
[21] Y. S. Hamed, M. Sayed, and A. A. Alshehri, "Active vibration suppression of a nonlinear electromechanical oscillator system with simultaneous resonance," *J. Vibroeng.*, vol. 20, no. 1, pp. 42–61, Feb. 2018.
[22] Y. S. Hamed and M. Sayed, "Stability analysis and response of nonlinear rotor-seal system," *J. Vibroeng.*, vol. 16, no. 8, pp. 4152–4170, 2014.
[23] M. Sayed and Y. S. Hamed, "Stability and response of a nonlinear coupled pitch-roll ship model under parametric and harmonic excitations," *Nonlinear Dyn.*, vol. 64, no. 3, pp. 207–220, May 2011.
[24] Y. S. Hamed, M. R. Alharthi, and H. K. AlKhathami, "Nonlinear vibration behavior and resonance of a Cartesian manipulator system carrying an intermediate end effector," *Nonlinear Dyn.*, vol. 91, no. 3, pp. 1429–1442, Feb. 2018.
[25] M. Sayed, A. A. Mousa, and I. Mustafa, "Stability and bifurcation analysis of a buckled beam via active control," *Appl. Math. Model.*, vol. 82, pp. 649–665, Jun. 2020.
[26] Y. S. Hamed, A. El Shehry, and M. Sayed, "Nonlinear modified positive position feedback control of cantilever beam system carrying an intermediate lumped mass," *Alexandria Eng. J.*, vol. 59, no. 5, pp. 3847–3862, Oct. 2020.
[27] A. Kandil, M. Sayed, and N. A. Saeed, "On the nonlinear dynamics of constant stiffness coefficients 16-pole rotor active magnetic bearings system," *Eur. J. Mech.-A/Solids*, vol. 84, Nov. 2020, Art. no. 104051.
[28] A. Kandil and H. El-Gohary, "Investigating the performance of a time delayed proportional–derivative controller for rotating blade vibrations," *Nonlinear Dyn.*, vol. 91, no. 4, pp. 2631–2649, Mar. 2018.
[29] A. Kandil and M. Kamel, "Vibration control of a compressor blade using position and velocity feedback," *Int. J. Acoust. Vib.*, vol. 24, no. 1, pp. 97–112, Mar. 2019.
[30] Y. Hamed, A. A. Aly, B. Saleh, A. F. Alogla, A. M. Aljuaid, and M. M. Alharthi, "Nonlinear structural control analysis of an offshore wind turbine tower system," *Processes*, vol. 8, no. 1, p. 22, Dec. 2019.
[31] Y. S. Hamed, A. A. Aly, B. Saleh, A. F. Alogla, A. M. Aljuaid, and M. M. Alharthi, "Vibration performance, stability and energy transfer of wind turbine tower via Pd controller," *Comput., Mater. Continua*, vol. 64, no. 2, pp. 871–886, 2020.
[32] Y. S. Hamed, H. Alotaibi, and E. R. El-Zahar, "Nonlinear vibrations analysis and dynamic responses of a vertical conveyor system controlled by a proportional derivative controller," *IEEE Access*, vol. 8, pp. 119082–119093, 2020.
[33] A. H. Nayfeh, *Problems in Perturbation*. New York, NY, USA: Wiley, 1985.
[34] A. H. Nayfeh, D. T. Mook, *Nonlinear Oscillations*. New York, NY, USA: Wiley, 1995.

Y. S. HAMED received the M.Sc. and Ph.D. degrees in mathematics from the Faculty of Science, Menoufia University, Egypt, in 2005 and 2009, respectively. Since 2009, he has been an Associate Professor of mathematics with the Mathematics and Statistics Department, Taif University, Saudi Arabia. He is currently an Associate Professor of engineering mathematics with the Department of Physics and Engineering Mathematics, Faculty of Electronic Engineering, Menoufia University. He supervised and examined some of M.Sc. and Ph.D. degree students. His research interests include the theory of differential equations and its application, numerical analysis, modeling, dynamical systems control, chaotic systems, renewable energy systems, and vibration control and computational methods for solving differential equations and engineering systems. He was an Editor of the *International Journal of Control, Automation and Systems* (IJCAS).

K. M. ALBOGAMY received the B.Sc. degree from Taif University, Saudi Arabia, in 2014. Her research interests include differential equations and dynamical systems.

M. SAYED received the B.Sc. degree in mathematics from Minia University, Egypt, in 1996, and the M.Sc. and Ph.D. degrees from Menoufia University, Egypt, in 2002 and 2006, respectively. He is currently a Professor and the Head of the Department of Physics and Engineering Mathematics, Faculty of Electronic Engineering, Menoufia University. His research interests include theory of differential equations and its application, numerical analysis, modeling, dynamical systems control, chaotic systems, renewable energy systems, and vibration control and computational methods for solving differential equations and engineering systems.